

MULTIFRACTALITY OF THE MULTIPLICATIVE AUTOREGRESSIVE POINT PROCESSES

B. KAULAKYS, M. ALABURDA, V. GONTIS AND T. MESKAUSKAS

*Institute of Theoretical Physics and Astronomy of Vilnius University,
A. Gostauto 12,
LT-01108 Vilnius, Lithuania
E-mail: kaulakys@itpa.lt*

Multiplicative processes and multifractals have earned increased popularity in applications ranging from hydrodynamic turbulence to computer network traffic, from image processing to economics. We analyse the multifractality of the recently proposed point process models generating the signals exhibiting $1/f^\beta$ noise. The models may be used for modeling and analysis of stochastic processes in different systems. We show that the multiplicative point process models generate multifractal signals, in contrast to the formally constructed signals with $1/f^\beta$ noise and signals consisting of sum of the uncorrelated components with a wide-range distribution of the relaxation times.

1. Introduction

Multifractal models are used to account for scale invariance properties of various objects in different domains ranging from the energy dissipation in turbulent flows¹ to financial data². Healthy human heartbeat intervals exhibit multifractal properties rather than being fractal for a life-threatening condition, known as congestive heart failure³. Cerebral blood flow in healthy humans is also multifractal⁴.

Scaling behavior has become a welcome careful description of complexity in many fields including natural phenomena, human heart rhythm in biology, spatial repartition of faults in geology, as well as human activities such as traffic in computer networks and financial markets. The multifractal formalism has received much attention as one of the most popular frameworks to describe and analyse signals and processes that exhibit scaling properties, covering and connecting both the local scaling and the global one in terms of sample moments.

The purpose of this paper is to analyse the multifractality of signals exhibiting $1/f^\beta$ noise generated by different techniques and, especially, of the point processes with $1/f^\beta$ power spectral density^{5,6}.

First of all, however, we will analyse the multifractality of the signal constructed by the inverse fast Fourier transform⁷. Using this method we can generate signals with any desirable slope β of the power spectral density $S(f) \sim 1/f^\beta$.

We calculate a generalized q th order height-height correlation function (GHCF)

$F_q(t)$ defined as⁸

$$F_q(t) = \langle |I(t' + t) - I(t')|^q \rangle^{1/q}, \quad (1)$$

where the angular brackets denote the time average. The GHCF $F_q(t)$ characterizes the correlation properties of the signal $I(t)$, and for a multifractal signal a power-law behavior like

$$F_q(t) \sim t^{H_q} \quad (2)$$

is expected. Here H_q is the generalized q th order Hurst exponent. If H_q is independent on q , a single scaling exponent H_q is involved and the signal $I(t)$ is said to be monofractal⁸. If H_q depends on q , the signal is considered to be multifractal.

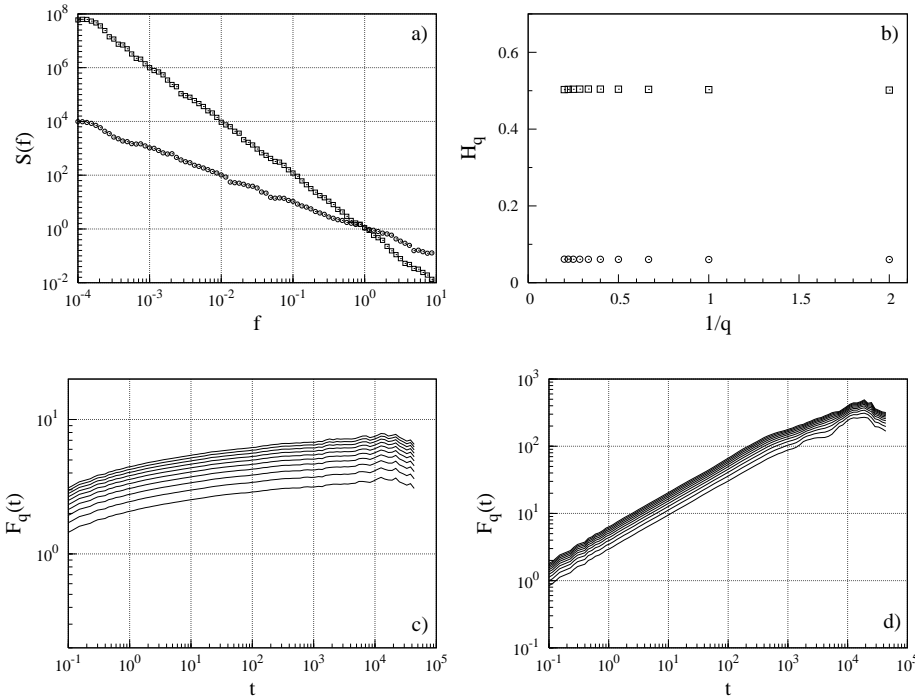


Figure 1. a) Power spectral density and b) the generalized Hurst exponents H_q versus $1/q$ in the scaling regime $1 < t < 1000$ for the slopes $\beta = 1$ (open circles) and $\beta = 2$ (open squares). The signal of 10^6 points was generated and averaged over 10 realizations. c) and d) show GHCF $F_q(t)$ versus time t for the same parameters $\beta = 1$ and $\beta = 2$, respectively.

In figure 1 a) we present a power spectral densities with the different slopes β and in figure 1 b) we show the Hurst exponents, calculated from GHCF using linear regression dependence on $1/q$ of the signals formally constructed by the inverse Fourier transform. In figure 1 c) and d) corresponding GHCF $F_q(t)$ versus time t are shown. We see that Hurst exponent H_q does not depend on q , which indicates that the signal is monofractal.

2. Stochastic multiplicative point process

In many cases the intensity of some signals or currents can be represented by a sequence of random (however, as a rule, mutually correlated) pulses or elementary events $A_k(t - t_k)$,

$$I(t) = \sum_k A_k(t - t_k). \quad (3)$$

Here the function $A_k(\phi)$ represents the shape of the k pulse making an influence on the signal $I(t)$ in the region of the transit time t_k . We will be interested in the processes with the power-law distribution of the power spectral density at low frequencies. It is easy to show that the shapes of the pulses mainly influence the high frequency, $f \gtrsim 1/\Delta t_p$, with Δt_p being the characteristic pulse length, power spectral density, while fluctuations of the pulse amplitudes result, as a rule, in the white or the Lorentzian but not $1/f$ noise⁹. Therefore, we restrict our analysis to noise due to correlations between the transit times t_k . In such approach we can replace the function $A_k(t - t_k)$ by the Dirac delta function and then express the signal as

$$I(t) = \bar{a} \sum_k \delta(t - t_k), \quad (4)$$

with \bar{a} being an average contribution to the signal of one pulse. This model⁵ also corresponds to the flow of identical objects: electrons, photons, cars, and so on, and is called the point process model. Point processes arise in different fields, such as physics, economics, cosmology, ecology, neurology, seismology, traffic flow, signaling and telecom networks, and the Internet (see e.g., papers^{9,10} and references herein).

The power spectrum of the point process signal is described completely by the set of the interevent intervals $\tau_k = t_{k+1} - t_k$. Moreover, the low frequency noise is defined by the statistical properties of the signal at a large-time-scale, i.e., by the fluctuations of the time difference

$$\Delta(k; q) \equiv t_{k+q} - t_k = \sum_{i=k}^{k+q-1} \tau_i \quad (5)$$

at large q , determined by the slow dynamics of the average interpulse time $\tilde{\tau}_k(q) = \Delta(k; q)/q$ between the occurrence of pulses k and $k + q$. Quite generally the dependence of the average interevent time $\tilde{\tau}_k$ may be described by the general Langevin equation. The Langevin equation may be written down in the actual time t or, equivalently, in the space of the occurrence numbers k with the drift coefficient $h(\tilde{\tau}_k)$ and a multiplicative noise $g(\tilde{\tau}_k)\xi(k)$,

$$\frac{d\tilde{\tau}_k}{dk} = h(\tilde{\tau}_k) + g(\tilde{\tau}_k)\xi(k). \quad (6)$$

Here we interpret k as a continuous variable while the white Gaussian noise $\xi(k)$ satisfies the standard condition

$$\langle \xi(k)\xi(k') \rangle = \delta(k - k') \quad (7)$$

with the brackets $\langle \dots \rangle$ denoting the averaging over the realizations of the process. We understand the equation (6) in Itô interpretation.

Transition from the occurrence numbers k to the actual time t in Eq. (6) may be fulfilled using the relation $dt = \tilde{\tau}_k dk$ ¹¹.

The particular sequence of the interevent times τ_k may be superimposed by some additional noise or stochasticity, e.g., τ_k may be determined by the Poisson distribution

$$P(\tau_k) = \frac{1}{\tilde{\tau}_k} e^{-\tau_k/\tilde{\tau}_k} \quad (8)$$

with the slowly, according to Eq. (6), changeable average interevent time $\tilde{\tau}_k$. Such additional stochasticity do not influence the long-range statistical properties and the low frequency spectra of the process. Therefore, further we will restrict the analysis to the processes generated by Eq. (6) and will identify τ_k with $\tilde{\tau}_k$.

2.1. Power spectral density

The point process is entirely defined by the occurrence times t_k . The power spectral density of the point process (4) may be expressed as

$$S(f) = \lim_{T \rightarrow \infty} \left\langle \frac{2}{T} \left| \int_{t_i}^{t_f} I(t) e^{-i2\pi f t} dt \right|^2 \right\rangle = \lim_{T \rightarrow \infty} \left\langle \frac{2\bar{a}^2}{T} \sum_k \sum_{q=k_{\min}-k}^{k_{\max}-k} e^{i2\pi f \Delta(k;q)} \right\rangle, \quad (9)$$

where t_i and t_f are initial and final observation times, $T = t_f - t_i \gg \omega^{-1}$ is the whole observation time and $\omega = 2\pi f$. Here k_{\min} and k_{\max} are minimal and maximal values of index k in the interval of observation T and the brackets $\langle \dots \rangle$ denote the averaging over realizations of the process.

For the interpulse intervals described by the Langevin equation (6) we use a perturbative solution in the vicinity of τ_k . After replacing the averaging over k by the averaging over the distribution $P_k(\tau_k)$ of the interpulse times τ_k , we have the power spectrum⁶

$$S(f) = 2\bar{I}^2 \frac{\bar{\tau}}{\sqrt{\pi}f} \int_0^\infty P_k(\tau_k) \operatorname{Re}[e^{-i(x-\frac{\pi}{4})} \operatorname{erfc} \sqrt{-ix}] \frac{\sqrt{x}}{\tau_k} d\tau_k, \quad (10)$$

where \bar{I} and $\bar{\tau}$ are the averages of the signal and the interpulse times, respectively, and $x = \pi f \tau_k^2 / h(\tau_k)$.

The replacement of the averaging over k and over realizations of the process by the averaging over the distribution of the interpulse times τ_k , $P_k(\tau_k)$, is possible when the process is ergodic. Ergodicity is usually a common feature of the stationary process described by the general Langevin equation.

According to Eq. (10) the small interpulse times and the clustering of the pulses make the greatest contribution to $1/f^\beta$ noise. The power-law spectral density is very often related with the power-law behavior of other characteristics of the signal,

such as autocorrelation function, probability densities and other statistics, and with the fractality of the signals, in general¹². Therefore, we investigate the power-law dependences of the drift coefficient and of the distribution density on the time τ_k in some interval of the small interpulse times, i.e.,

$$h(\tau_k) = \gamma \tau_k^\delta, \quad P_k(\tau_k) = C \tau_k^\alpha, \quad \tau_{\min} \leq \tau_k \leq \tau_{\max}, \quad (11)$$

where the coefficient γ represents the rate of the signal's nonlinear relaxation and C has to be defined from the normalization.

The simplest and the well-known process generating the power-law probability distribution function for τ_k is a multiplicative stochastic process with $g(\tau_k) = \sigma \tau_k^\mu$ and $\delta = 2\mu - 1$, written as^{6,13}

$$\tau_{k+1} = \tau_k + \gamma \tau_k^{2\mu-1} + \sigma \tau_k^\mu \varepsilon_k. \quad (12)$$

Here γ represents the nonlinear relaxation of the signal, while τ_k fluctuates due to the perturbation by normally distributed uncorrelated random variables ε_k with a zero expectation and unit variance and σ is a standard deviation of the white noise.

Eq. (12) is the difference (discrete) version of the differential equation (6). On the other hand, it is the generalization of the simple autoregressive model of $1/f$ noise⁵ (see also Eq. (15)) and represents quite general evolution of the interevent time with the nonlinear drift $h(\tau_k) = \gamma \tau_k^{2\mu-1}$ and the multiplicative noise $\sigma \tau_k^\mu \varepsilon_k$, resulting in the $1/f^\beta$ noise and power-law distribution (11) of the interevent time τ_k with the exponent $\alpha = 2\gamma/\sigma^2 - 2\mu$. Indeed, the power spectrum for the process (12), when $\gamma/(\pi \tau_{\max}^{2-\delta}) \ll f \ll \gamma/(\pi \tau_{\min}^{2-\delta})$, is⁶

$$S(f) = \frac{(2+\alpha)(\beta-1)\bar{a}^2 \Gamma(\beta-1/2)}{\sqrt{\pi} \alpha (\tau_{\max}^{2+\alpha} - \tau_{\min}^{2+\alpha}) \sin(\pi\beta/2)} \left(\frac{\gamma}{\pi}\right)^{\beta-1} \frac{1}{f^\beta}, \quad (13)$$

where

$$\alpha = \frac{2\gamma}{\sigma^2} - 2\mu, \quad \beta = 1 + \frac{\alpha}{3-2\mu}, \quad \frac{1}{2} < \beta < 2. \quad (14)$$

For $\mu = 1$ we have a completely multiplicative point process when the stochastic change of the interpulse time is proportional to itself. Another case of interest concerns $\mu = 1/2$, then we have the Brownian motion of the interevent time with the linear relaxation of the signal $I \simeq \bar{a}/\tau$.

Figure 2 represents the spectral densities (9) with different slopes β of the signals generated numerically according to Eqs. (4) and (12) for different parameters of the model. We see that the simple iterative equation (12) with the multiplicative noise produces the signals with the power spectral density of different slopes, depending on the parameters of the model. The agreement of the numerical results with the approximate theory is quite good.

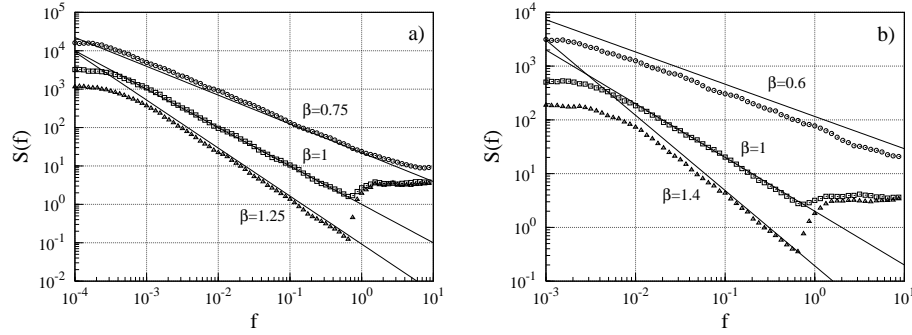


Figure 2. Power spectral density (9) vs frequency of the signal generated by Eqs. (4) and (12) with the parameters a) $\mu = 0.5$, $\sigma = 0.02$ and different relaxations of the signal $\gamma = 0.0001$ (open circles), 0.0002 (open squares) and 0.0003 (open triangles); and b) $\mu = 1$, $\sigma = 0.1$ and $\gamma = 0.008$ (open circles), 0.01 (open squares) and 0.012 (open triangles). We restrict the diffusion of the interevent time in the interval $\tau_{\min} = 10^{-6}$, $\tau_{\max} = 1$ with the reflective boundary condition at τ_{\min} and transition to the white noise, $\tau_{k+1} = \tau_{\max} + \sigma \varepsilon_k$, for $\tau_k > \tau_{\max}$ and 100 realizations with 10^6 t_k points each were used. The solid lines represent the analytical results according to Eq. (13).

2.2. Multifractal point processes

The multifractal formalism has received much attention recently as one of the most popular frameworks to describe and analyse signals and processes that exhibit the scaling properties.

Fractality of the point process can be investigated by transition from the point process to the stochastic signal $I(t)$, using the rectangular constant area pulses, instead of the Dirac delta functions. The stochastic signal will have the same fractal properties as the origin point process.

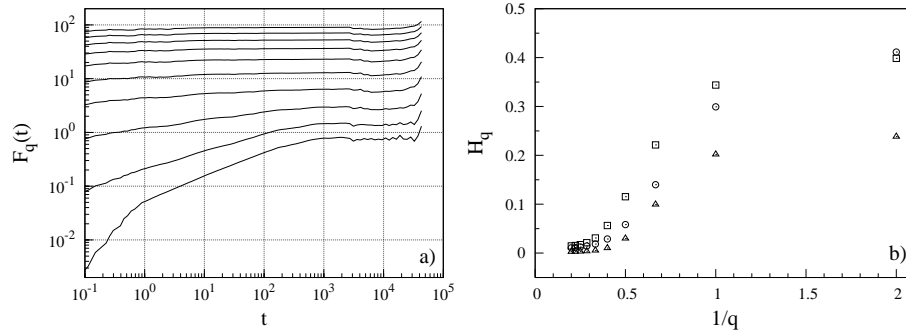


Figure 3. a) Generalized height-height correlation function $F_q(t)$ versus time t for the signal (4) and (12) with $\mu = 0.5$, $\bar{\tau} = 1$, $\sigma = 0.02$, $\gamma = 0.0002$, and $q = 0.5, 1, 1.5, \dots, 5$ from bottom to top. b) The generalized Hurst exponents H_q versus $1/q$ in the scaling regime $1 < t < 1000$ for the $\bar{\tau} = 1$ and $\mu = 0.5$, $\sigma = 0.02$, $\gamma = 0.0002$ (open circles); $\mu = 0.5$, $\sigma = 0.02$, $\gamma = 0.0003$ (open squares); $\mu = 1$, $\sigma = 0.1$, $\gamma = 0.008$ (open triangles).

In figure 3 a) we present the GHCF as a function of the time interval t , and in figure 3 b) we show the Hurst exponents calculated from GHCF using the linear regression dependence on $1/q$ for different parameters μ , σ , and γ . We observe the clear multifractal behavior since the slopes of the log-log plot of GHCF are depending on q .

Another interesting case is a sequence of transit times with random increments of the time intervals between pulses, $\tau_k = \tau_{k-1} + \sigma \varepsilon_k$. It is natural to restrict in some way the infinite Brownian increase or decrease of the interpulse times τ_k , e.g., by the introduction of the relaxation to the average interpulse time $\bar{\tau}$ rate γ . So, we have an additive point process

$$\tau_k = \tau_{k-1} - \gamma(\tau_{k-1} - \bar{\tau}) + \sigma \varepsilon_k. \quad (15)$$

This model generates the process with $1/f$ noise⁵, and may be useful for modeling and analysing different systems (see references in paper⁶). Introduction of the reflective boundary condition at $\tau_{\min} > 0$ avoids the formation of clusters and leads to $1/f^2$ noise.

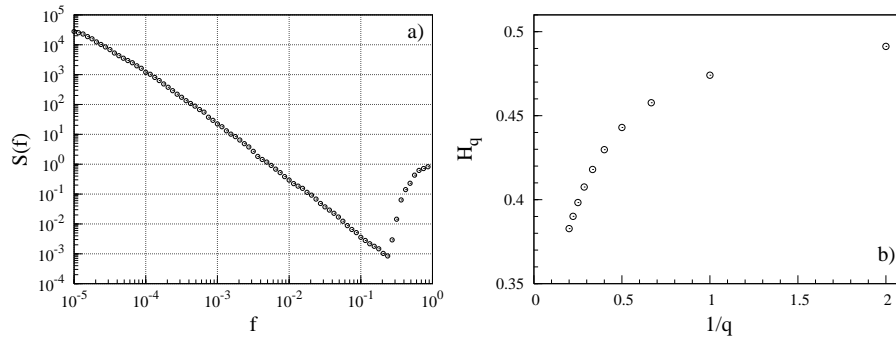


Figure 4. a) Power spectral density and b) the generalized Hurst exponents of the additive point process (15) with the reflecting boundary condition at $\tau_{\min} = 0.1$ in the scaling regime $1 < t < 1000$. The signal of 10^6 points was generated with the parameters $\bar{\tau} = 1$, $\sigma = 0.001$, and $\gamma = 0.000001$.

In figure 4 a) we present a power spectral density of the additive point process (15) with the reflecting boundary condition and in figure 4 b) we show the generalized Hurst exponents. We observe the multifractal behavior of the additive point process.

2.3. Monofractality of the white and the Gaussian noises

It is well-known⁹ that the point processes with the interevent time τ_k distributed according to Poisson distribution

$$P(\tau_k) = \frac{1}{\bar{\tau}} e^{-\tau_k/\bar{\tau}} \quad (16)$$

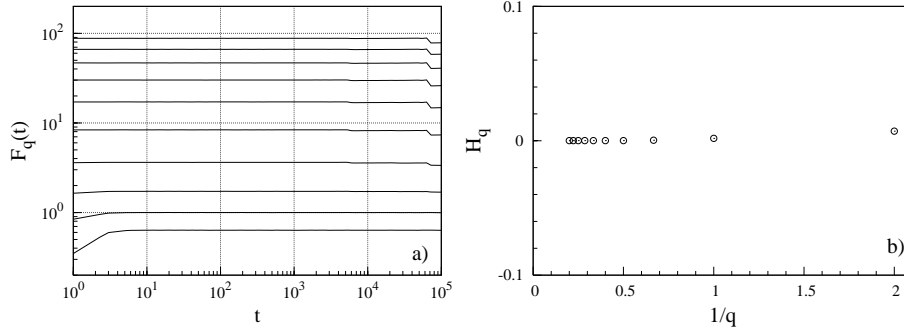


Figure 5. a) Generalized height-height correlation function $F_q(t)$ versus time t , and b) the generalized Hurst exponents H_q versus $1/q$ of the point process with interevent time τ_k distributed according to Poisson distribution (16) in the scaling regime $1 < t < 1000$. The signal of 10^6 points with the parameter $\bar{\tau} = 1$ has been generated.

generate the white noise, $S(f) = \text{const.}$

In figure 5 a) we present the GHCF as a function of the time interval t and in figure 5 b) we show the Hurst exponents for the white noise. The Hurst exponents of the white noise are equal to zero. This demonstrates the absence of the scaling and that there is no correlation in time.

Noise with the power-law spectral density $1/f$ is often modeled as the sum of the Lorentzian spectra with the appropriate weights of a wide range distribution of the relaxation times τ^{rel} . The signal may be expressed as a sum of N uncorrelated components,

$$I(t) = \sum_{l=1}^N I_l(t) = \int_{\gamma_{\min}}^{\gamma_{\max}} I(t, \gamma) g(\gamma) d\gamma, \quad (17)$$

where $g(\gamma)$ is the distribution of the relaxation rates $\gamma = 1/\tau^{rel}$, and every component I_l satisfies the stochastic differential equation

$$\dot{I}_l = -\gamma_l(I_l - \bar{I}_l) + \sigma_l \xi_l(t). \quad (18)$$

Here \bar{I}_l is the average value of the signal component I_l , $\xi_l(t)$ is the δ -correlated white noise, $\langle \xi_l(t) \xi_{l'}(t') \rangle = \delta_{l,l'} \delta(t - t')$, and σ_l is the intensity (standard deviation) of the white noise. The steady-state solution of the stationary Fokker-Planck equation corresponding to Eq. (18) for each component I_l and the resulting signal (17) yields the Gaussian distribution densities, however, the power spectrum may be of the power-law form when $\sigma^2(\gamma)g(\gamma)$ is constant or a power-law function⁶.

In figure 6 a) we present a power spectral density of the sum of the signals with a wide range distribution of the relaxation times τ^{rel} and in figure 6 b) we show the Hurst exponents, calculated from GHCF using linear regression dependence on $1/q$. In the figures we observe $1/f$ behavior of the signal noise and clearly see that Hurst exponent H_q does not depend on q , which shows that the signal (17) is monofractal.

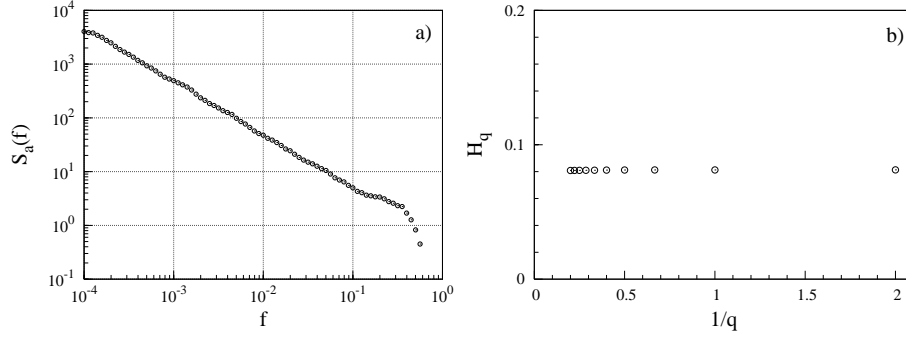


Figure 6. a) Power spectral density and b) the generalized Hurst exponents H_q versus $1/q$ in the scaling regime $1 < t < 1000$. The signal of 10^6 points was generated from 10 components with the parameters $\bar{I} = 20$, $\sigma^2(\gamma)g(\gamma) = 10$, and uniform distribution of $\lg \gamma$ with γ values in the interval $10^{-4} - 1$.

3. Conclusions

The multiplicative (12) and additive (15) stochastic point processes may generate time series exhibiting the power spectral density $S(f) \sim 1/f^\beta$ and show clear multifractal behavior, however, the formally constructed by the inverse Fourier transform signal, Poisson white noise (16) and Gaussian, Eqs. (17) and (18), signal with the power spectral density $S(f) \sim 1/f$ are monofractal.

Therefore, the proposed⁵ and generalized⁶ point process models of $1/f^\beta$ noise may be used for modeling of stochastic multifractal processes in different systems.

Acknowledgments

We acknowledge support by the Lithuanian State Science and Studies Foundation and EU COST Action P10 “Physics of Risk”.

References

1. U. Frisch, *Turbulence: The Legacy of A. N. Kolmogorov*, Cambridge University Press (1995).
2. J.-P. Bouchaud and M. Potters, *Theory of Financial Risk and Derivative Pricing*, Cambridge University Press (1999).
3. P. C. Ivanov, M. G. Rosenblum, L. A. N. Amaral, Z. R. Struzik, S. Havlin, A. L. Goldberger, and H. E. Stanley, *Nature* **399**, 461 (1999); P. C. Ivanov, L. A. N. Amaral, A. L. Goldberger et al., *Chaos* **11**, 641 (2001).
4. B. J. West, M. Latka, M. Glaubic-Latka, and D. Latka, *Physica A* **318**, 453 (2003).
5. B. Kaulakys and T. Meškauskas, *Phys. Rev. E* **58**, 7013 (1998); B. Kaulakys, *Phys. Lett. A* **257**, 37 (1999).
6. B. Kaulakys, V. Gontis, and M. Alaburda, *Phys. Rev. E* **71**, 051105 (2005).
7. J. Timmer and M. König, *Astron. Astrophys.* **300**, 707 (1995).
8. P. Meakin, *Fractals, Scaling and Growth Far From Equilibrium*, Cambridge University Press (1998); E. Bacry, J. Delour, and J. F. Muzy, *Phys. Rev. E* **64**, 026103 (2001);

- D.R. Bickel, *Fractals* **11**, 245 (2003); J. W. Lee, K. E. Lee, and P. A. Rikvold, arXiv: nlin/0412038 (2004).
9. T. Lukes, *Proc. Phys. Soc.* **78**, 153 (1961); C. Heiden, *Phys. Rev.* **188**, 319 (1969); K. L. Schick and A. A. Verveen, *Nature* **251**, 599 (1974).
 10. S. Thurner, S. B. Lowen, M. C. Feurstain et al., *Fractals* **5**, 565 (1997); L. Telesca, V. Cuomo, V. Lapenna, and M. Macchiato, *Fluct. Noise Lett.* **2**, L357 (2002); T. Musha and H. Higuchi, *Jap. J. Appl. Phys.* **15**, 1271 (1976); A. J. Field, U. Harder, and P. G. Harrison, *IEE Proceedings-Communications* **151**, 355 (2004); I Csabai, *J. Phys. A* **27**, L417 (1994); F. Grüneis, *Physica A* **123**, 149 (1984); T. Musha and K. Shimizu, *Jap. J. Appl. Phys.* **26**, 2022 (1987); M. Y. Choi and H. Y. Lee, *Phys. Rev. E* **52**, 5979 (1995); F. Grüneis, *Fluct. Noise Lett.* **1**, R119 (2001); J. M. Halley and P. Inchausti, *Fluct. Noise Lett.* **4**, R1 (2004).
 11. B. Kaulakys and J. Ruseckas, *Phys Rev. E* **70**, 020101 (R) (2004).
 12. B. B. Mandelbrot, *Multifractals and 1/f Noise*, Springer-Verlag (1999); B. B. Mandelbrot, *Fractals and Scaling In Finance*, Springer-Verlag (1997); R. N. Mantegna and H. E. Stanley, *An Introduction to Econophysics: Correlations and Complexity in Finance*, Cambridge University Press (1999); X. Gabaix, P. Gopikrishnan, V. Plerou, and H. E. Stanley, *Nature* **423**, 267 (2003).
 13. V. Gontis and B. Kaulakys, *Physica A* **343**, 505 (2004); V. Gontis and B. Kaulakys, *Physica A* **344**, 128 (2004).